Dev Genes Evol (1996) 206:180–194

ORIGINAL ARTICLE

Lewis I. Held Jr · Michael A. Heup

Genetic mosaic analysis of *decapentaplegic* and *wingless* gene function in the *Drosophila* leg

Received: 25 March 1996 / Accepted: 13 June 1996

Abstract Genetically mosaic flies were constructed which lack a functional *decapentaplegic* (*dpp*) or *wingless* (*wg*) gene in portions of their leg epidermis, and the leg cuticle was examined for defects. Although *dpp* has previously been shown to be transcribed both ventrally and dorsally, virtually the only *dpp*-null clones that affect leg anatomy are those which reside dorsally. Conversely, *wg*-null clones only cause leg defects when they reside ventrally – a result that was expected, given that *wg* is only expressed ventrally. Both findings are consistent with models of leg development in which the future tip of the leg is specified by an interaction between *dpp* and *wg* at the center of the leg disc. Null clones can cause mirror-image cuticular duplications confined to individual leg segments. Double-ventral, mirror-image patterns are observed with *dpp*-null clones, and double-dorsal patterns with *wg*-null clones. Clones that are doubly mutant (null for both *dpp* and *wg*) manifest reduced frequencies for both types of duplications. Duplications can include cells from surrounding non-mutant territory. Such nonautonomy implies that both *dpp* and *wg* are involved in positional signaling, not merely in the maintenance of cellular identities. However, neither gene product appears to function as a morphogen for the entire leg disc, since the effects of each gene's null clones are restricted to a discrete part of the circumference. Interestingly, the circumferential domains where *dpp* and *wg* are needed are complementary to one another.

Key words Positional information · Pattern formation · *decapentaplegic* · *wingless* · Leg

Introduction

Ever since Lewis Wolpert's seminal paper on positional information (Wolpert 1969), developmental biologists have become cartographers, looking for chemical grids that might enable cells to discern their locations within organs. Many organs seem to have poles, like the earth's north and south poles, that define various reference axes. The legs of the fruitfly *Drosophila melanogaster* are prime examples. Each of them develops from an imaginal disc shaped like a deflated balloon (Fig. 1; Bryant 1978; Cohen 1993). A single line bisects the disc into an anterior and a posterior cell lineage compartment (Steiner 1976). Anterior cells express the gene *cubitus-interruptus*, whereas posterior cells express *engrailed* and *hedgehog* (reviewed by Held 1995). In the center of this line is a point which will become the tip of the leg when the disc telescopes out during metamorphosis. The "poles" of the leg appear to reside on either side of this point. Dorsally, just anterior to the compartment boundary, lies a sector where *decapentaplegic* (*dpp*) is transcribed, and ventrally there is a sector where *wingless* (*wg*) is transcribed along with *dpp*, though *dpp* transcription there is weaker than it is dorsally, at least during the third instar (Masucci et al. 1990).

Hypomorphic mutations in *dpp* and *wg* can cause "duplication-deficiency" phenotypes, where the leg manifests a mirror-image ventral (V/V) or dorsal (D/D) pattern respectively (Spencer et al. 1982; Baker 1988b; Bryant 1988; Peifer et al. 1991, Held et al. 1994). Such phenotypes suggest that these genes encode a dorsal-ventral coordinate of positional information in the disc (Held 1995). Other evidence for such a role has come from experiments where one or the other gene has been forced to be ectopically expressed at or near the "wrong" pole (*dpp* on the ventral side or *wg* on the dorsal side), which can cause dorsal-ventral duplications with or without leg bifurcations (Campbell et al. 1993; Struhl and Basler 1993; Diaz-Benjumea et al. 1994). The latter kinds of experiments have led to a model for leg development in which the *dpp* and *wg* gene products are supposed to interact at the center of the disc to specify the tip of the leg and cause distal outgrowth (Campbell et al. 1993; Campbell and Tomlinson 1995). In order for this "Distal Organizer" Model to work, it has been necessary to assume

Edited by D. Tautz

L.I. Held Jr (✉) · M.A. Heup
Department of Biological Sciences, Texas Tech University, Lubbock, Texas 79409, USA

that the ventral domain of *dpp* expression is irrelevant for leg patterning. (Otherwise, *dpp* and *wg* would interact ventrally to cause multiple outgrowths.) Until now, however, this assumption has not been directly tested. The current investigation was undertaken to test this conjecture, i.e. to determine whether *dpp* function is needed ventrally. Our results argue that it is not. Hence, the conjecture appears correct.

In order to find the regions of the leg where the *dpp* and *wg* gene products are essential, mitotic recombination was utilized to homozygose null alleles in cell clones that were also marked with bristle color mutations (cf. Postlethwait 1978). If a null clone happens to overlap an area where the gene's function is required in patterning, then the cuticular pattern should be abnormal. By: (1) examining enough randomly located clones to collectively saturate the entire leg circumference and (2) charting which sectors show abnormalities, we were able to identify the parts of the disc where *dpp* and *wg* activity are needed. The *dpp* and *wg* genes are respectively needed along the dorsal and ventral midlines, consistent with their areas of maximal transcription. Although *dpp* is also transcribed at a reduced level along the ventral midline, it is apparently not needed there since *dpp*-null clones in that region have virtually no effect on leg anatomy. A similar conclusion was implied by gynandromorph mosaic studies where a hypomorphic *dpp* genotype (dpp^{d6}/dpp^{d14}) was used instead of a null one (Spencer 1984). However, this result contrasts with the findings of a similar mosaic analysis in the wing: in the wing disc, *dpp* is apparently needed along its entire stripe of expression, both dorsally and ventrally (Posakony et al. 1991).

Materials and methods

Induction of mitotic-recombination clones

Two different approaches were utilized to produce mosaic flies (cf. Blair 1995a). The first (crosses #1–5) employed "*FLP-FRT*" site-specific recombination. Heat shocks were used to activate a heat-shock promoter coupled to a site-specific "*FLP*" recombinase (Golic 1991) whose targets are "*FRT*" sequences. In our stocks the *FRT* sites are at the base (region 40A) of the left arm of the second chromosome (Xu and Rubin 1993). Segregation of recombinant homologues can: (1) homozygose all genes distal to the *FRT* inserts, (2) remove a $yellow^+$ gene at 25F, and hence (3) mark a daughter cell and its descendents with *yellow* (*y*) which causes yellowish bristles. In each experiment, a single heat shock was administered for 1 h at 38°C by partially submerging 10-dram plastic vials (containing food and larvae) in a covered water bath.

The second method was intended to remove all *dpp* genes from the marked cell and to maximize the size of the dpp^{null} clones. A 1,000 r (Cs^{137} source, 893 r/min) dose of gamma rays was used to induce crossing over in larvae heterozygous (*M*/+) for a *Minute* mutation that slows the rate of mitosis. In this "*Minute* technique" (Morata and Ripoll 1975) recombination liberates the +/+ daughter cell from the *Minute* impediment, allowing its progeny to divide faster than the background cells, producing a larger-than-normal clone. In cross #6, recombination proximal to the marker mutations *straw* (*stw*) and *pawn* (*pwn*) ejects not only the *Minute* but also the two duplications of the wild-type dpp^+ gene, leading to a fast-growing clone that lacks any *dpp* genes.

Both genetic schemes ensure that marked clones are homozygous for the *dpp*-null and/or *wg*-null alleles of interest, i.e. no gratuitously marked, non-mutant clones should be induced. The first method guarantees this result because recombination is directed to the 40A site, and all relevant genes are distal to it. In the second method, recombination can occur anywhere along the chromosome arm, but the proximal location of *stw* and *pwn* assures that clones marked with *stw* and *pwn* must also be *dpp*-null, barring rare double cross-overs. Three different *dpp*-null genotypes were used. The advantage of using multiple approaches is that each provides a control for genetic idiosyncracies of the others: clones induced by γ-rays versus *FLP-FRT* recombination can produce different phenotypes (Tabata et al. 1995). The *wg*-null allele that was used is wg^{CX4}, a deletion at the 5′ end of the *wg* gene which prevents any *wg* transcript (Baker 1987).

Fly strains and crosses

The two genes that were analyzed here are both on the left arm of the second chromosome: *dpp* at 4.0 and *wg* at 30.0 (salivary chromosome band locations 22F1-2 and 28A1-3 respectively). See Lindsley and Zimm (1992) for further information on these and other genes. The crosses listed below yielded F_1 heterozygotes capable of undergoing mitotic recombination to produce marked homozygous clones. "P" denotes a transposon whose genes are bracketed and whose insertion site is given after the brackets. "*MKRS, FLP^{48}*" is a third-chromosome balancer, *Tp(3;3)MKRS, M(3)76A, kar ry^2 Sb*, into which a recombinase-bearing *P[ry^+ hsFLP]* element was inserted (Chou and Perrimon 1992). The presence of this balancer was tracked via its dominant, bristle-thickening mutation *Stubble* (*Sb*). The effects of *Sb* are negligible for tarsal bristles, which is important since we used bristle thickness as an indicator of dorsal versus ventral identity in this region. *SM5* is a balancer tagged with the dominant wing-curling mutation *Curly* (*Cy*). Because the *Cy* phenotype is not detectable in pharate adults, we could not identify balancer from non-balancer (nonmosaic) F_1 individuals that died prior to eclosion. Hence, we only studied eclosed adults. Omission of rare dead pharates had little effect on the frequencies of abnormalities since adults could eclose despite leg deformities. Many legs in every series (≥ 10%) had ≤ 5 marked bristles per leg. The small size of the clones implies that they arise late in development (cf. Stern 1936; Held 1979b), and their presence in untreated controls (40 out of 194 Cross-#1 legs) indicates that they arise spontaneously. Hence, only legs bearing ≥ 6 marked bristles were tallied as "mosaic". In clone genotypes below, boldface denotes the homozygosed chromosome arm:

1. Control (dpp^+ wg^+) clones: ♀♀ *y; P[ry^+; hs-neo; FRT]40A/SM5* X ♂♂ *y; P[ry^+; y^+]25F, P[ry^+; hs-neo; FRT]40A; MKRS, FLP^{48}* → heat-shocked F_1, from which *Sb*, non-*Cy* ♂♂ were chosen (concise genotype: *y; FRT/y^+ FRT; Sb FLP/+*) for leg dissection and mounting. Clone genotype: *y;* **FRT/FRT***; Sb FLP/+*.
2. dpp^{d12} clones: ♀♀ *y; dpp^{d12}P[ry^+; hs-neo; FRT]40A/In(2LR)Gla* X ♂♂ *y; P[ry^+; y^+]25F, P[ry^+; hs-neo; FRT]40A; MKRS, FLP^{48}* → heat-shocked F_1, from which *Sb*, non-*Gla* ♂♂ were chosen (*y; dpp^{d12}FRT/y^+FRT; Sb FLP/+*). Clone genotype: *y;* **dpp^{d12} FRT/dpp^{d12} FRT***; Sb FLP/+*.
3. wg^{null} clones: ♀♀ *y; wg^{CX4}P[ry^+; hs-neo; FRT]40A/SM5* X ♂♂ *y; P[ry^+; y^+]25F, P[ry^+; hs-neo; FRT]40A; MKRS, FLP^{48}* → heat-shocked F_1, from which *Sb*, non-*Cy* ♂♂ were chosen (*y; wg^{CX4}FRT/y^+FRT; Sb FLP/+*). Clone genotype: *y;* **wg^{CX4} FRT/wg^{CX4} FRT;** *Sb FLP/+*.
4. Doubly mutant dpp^{d12} wg^{null} clones: ♀♀ *y; $dpp^{d12}wg^{CX4}$P[ry^+; hs-neo; FRT]40A/SM5* X ♂♂ *y; P[ry^+; y^+]25F, P[ry^+; hs-neo; FRT]40A; MKRS, FLP^{48}* → heat-shocked F_1, from which *Sb*, non-*Cy* ♂♂ were chosen (*y; $dpp^{d12}wg^{CX4}$FRT/y^+FRT; Sb FLP/+*). Clone genotype: *y;* **dpp^{d12} wg^{CX4} FRT/dpp^{d12} wg^{CX4} FRT***; Sb FLP/+*.
5. dpp^{null} "embryonic rescue" clones (*FLP-FRT* method): ♀♀ *y; P[ry^+; y^+]25F, P[ry^+; hs-neo; FRT]40A; MKRS, FLP^{48}* X ♂♂ *w; dpp^{H46} P[ry^+; hs-neo; FRT]40A/In(2LR)Gla; P[20Kb, ry^+]/+* →

Table 1 Frequencies of mosaic legs and abnormal leg segments

Cross	Clones		Legs		Leg Segments (Nos.) Abn. Dorsal			Abn. Ventral		
	Genotype	Stage when induced	Total	No. mosaic (% of total)	V/V	V/-	Tot.	D/D	D/-	Tot.
1	*dpp*$^{+}$ *wg*$^{+}$ (FLP control)	1st instar	1000	191 (19%)	0	0	0	0	0	0
1	*dpp*$^{+}$ *wg*$^{+}$ (FLP control)	2nd instar	700	196 (28%)	0	0	0	0	0	0
6	*dpp*$^{+}$ *wg*$^{+}$ (γ-ray control)	2nd instar	1000	23 (2%)	0	0	0	0	0	0
6	*dpp*$^{null\text{-}M+}$	2nd instar	2500	73 (3%)	8	10	18	0	0	0
5	*dpp*$^{null\text{-}ER}$	1st instar	2000	215 (11%)	0	26	26	0	3	3
2	*dpp*^{d12}	1st instar	1000	208 (21%)	21	8	29	0	0	0
3	*wg*^{null}	1st instar	2000	223 (11%)	0	0	0	35	1	36
4	*dpp*^{d12} *wg*^{null}	1st instar	1400	225 (16%)	5	9	14	15	4	19

Data are from second legs of males, except for γ-ray controls, which were sibling females. See Materials and methods for details about crosses, clone induction procedures, etc. Abnormally patterned leg segments are classified according to the part of the circumference that is abnormal. In the "Abnormal Dorsal" category the "V/V" subclass includes segments that have ventral-type bristles on their dorsal side, though few of these segments have a completely ventralized pattern in their dorsal half. Segments whose dorsal side contains gaps in addition to V-type bristles (see Fig. 2 key) are also tallied under the "V/V" heading. The "V/-" subclasss includes segments lacking portions of the dorsal bristle pattern but not displaying any ectopic V-type bristles on that side. Corresponding subclasses are indicated for the "Abnormal Ventral" category. Note: the six columns on the right concern leg segments, not whole legs. For each row, the sample size of leg segments equals nine times the number of mosaic legs (minus segments missing due to rare leg truncations). All 77 mosaic legs that contained dorsally or ventrally abnormal segments are schematically diagrammed in Fig. 2

heat-shocked F_1, from which *Sb*, non-*Gla* ♂♂ were chosen (*y; dpp*^{H46}*FRT/y*$^{+}$*FRT; P[20Kb]/Sb FLP*). "*P[20Kb]*" is a P-element transposon (inserted into a third chromosome) which carries 20 kb of DNA from the *dpp* gene region (Hursh et al. 1993). The 20 kb piece includes the *dpp* structural gene and its embryonic enhancers, but none of the 3′ enhancers that drive *dpp* expression in discs. The rationale for using this "embryonic rescue" transposon is explained in the Results. Clone genotype: *y;* **dpp^{H46} FRT/dpp^{H46} FRT***; P[20Kb]/Sb FLP*.

6. *dpp*^{null} clones (*Minute* method): ♀♀ *dpp*^{H48} *Dp(2;2)dpp*^{d21} *Dp(2;2)DTD48 M(2)60E / In(2LR)SM6a, Cy* X ♂♂ *Dp(2;1)G146, dpp*$^{+}$ */ Y*; *Df(2L)DTD2, dpp*$^{-}$ *stw pwn cn / In(2LR)CyO, Cy*; *mwh / mwh* → irradiated F_1, from which we picked non-*Cy* ♂♂ of the genotype *dpp*^{H48} · *stw*$^{+}$ *pwn*$^{+}$ *Dp(2;2)dpp*^{d21} *Dp(2;2)DTD48 M(2)60E / Df(2L)DTD2, dpp*$^{-}$ · *stw pwn cn; mwh / +*. "·" marks the centromere in the order of genes along the second chromosome. This is the same scheme used by Posakony et al. (1991; see their Fig. 2); *dpp*^{H48} behaves as a null for all *dpp* functions (St. Johnston et al. 1990). Crossovers to the right of the centromere will homozygose the right arm if they occur proximal to *stw*. Crossovers distal to *stw* would not produce detectable clones. Thus, all *stw*-marked clones in males should be *dpp*^{null}, barring double crossovers. Clone genotype: *dpp*^{H48} · **stw pwn***/Df(2L)DTD2, dpp*$^{-}$ · **stw pwn***; mwh/+*.

Rearing of flies and inspection of legs

Flies were raised on *Drosophila* Instant Medium (Ward's) prepared with a 0.1% aqueous solution of the mould inhibitor Tegosept M, plus live yeast on top of the food. Except during heat shocks, flies were maintained at 25°C. Eggs were collected from parents during 24-h periods ("AEL" = After Egg Laying) and aged for either 24 or 48 h to yield cohorts of first-instar (range of larval ages: 24–48 h AEL) or second-instar (age range: 48–72 h AEL) larvae, at which time either a 1-h 38°C heat shock or a 1,000 r dose of γ-irradiation was administered. To prevent overcrowding, larvae were transferred from egg-collection vials to fresh food bottles before mid-third instar. To prevent leg deformities from causing flies to stick to food, either (1) the food surface was covered with a tissue after larvae pupariated, or (2) pupae were transferred to humidified empty vials. Forceps were used to remove second legs in pairs, which were then placed in a drop of Faure's solution (Lee and Gerhart 1973) between cover slips. Legs were scanned for clones at × 200 magnification, and marked bristles were identified at × 400 using an Olympus BH-2 compound microscope at low contrast to accentuate bristle color differences.

Results

Preliminary studies of *FLP-FRT*-induced mosaicism

To investigate how *dpp* and *wg* function in leg development, we induced marked clones in young larvae (Table 1). Though the cuticular patterns of all three pairs of legs are similar (Hannah-Alava 1958), we only studied second legs because their distinctive dorsal and ventral bristles are ideal indicators of cellular identities. Dorsally there are the trochanteral edge bristle and the tibial preapical bristle; ventrally there are the tibial apical bristle and the tarsal peg-like bristles (Fig. 1).

Among 11,600 second legs examined for the presence of marked bristles, 1,354 mosaic legs were recovered. Strangely, mosaic legs induced by the *FLP-FRT* method (see Materials and methods) routinely had multiple stripes of marked bristles, rather than the single longitudinal stripe that is canonical for γ-ray-induced mosaics (Tokunaga 1962; Bryant and Schneiderman 1969; Held 1979b), and the stripes were often fragmented and irregular. To determine whether the multiple stripes are due to cross-overs in multiple founder cells, we tested whether individual legs have a higher-than-expected frequency of marked bristles in both the anterior and posterior leg compartments (A.C. and P.C.; Fig. 1b). Because cell lineages in the A.C. and P.C. are separated before the first instar (Steiner 1976), marked bristles in both compartments of a single leg must indicate a minimum of two clonal founder cells (one in the A.C. and one in the P.C.). In controls heat-shocked in the first-instar (cross #1: see

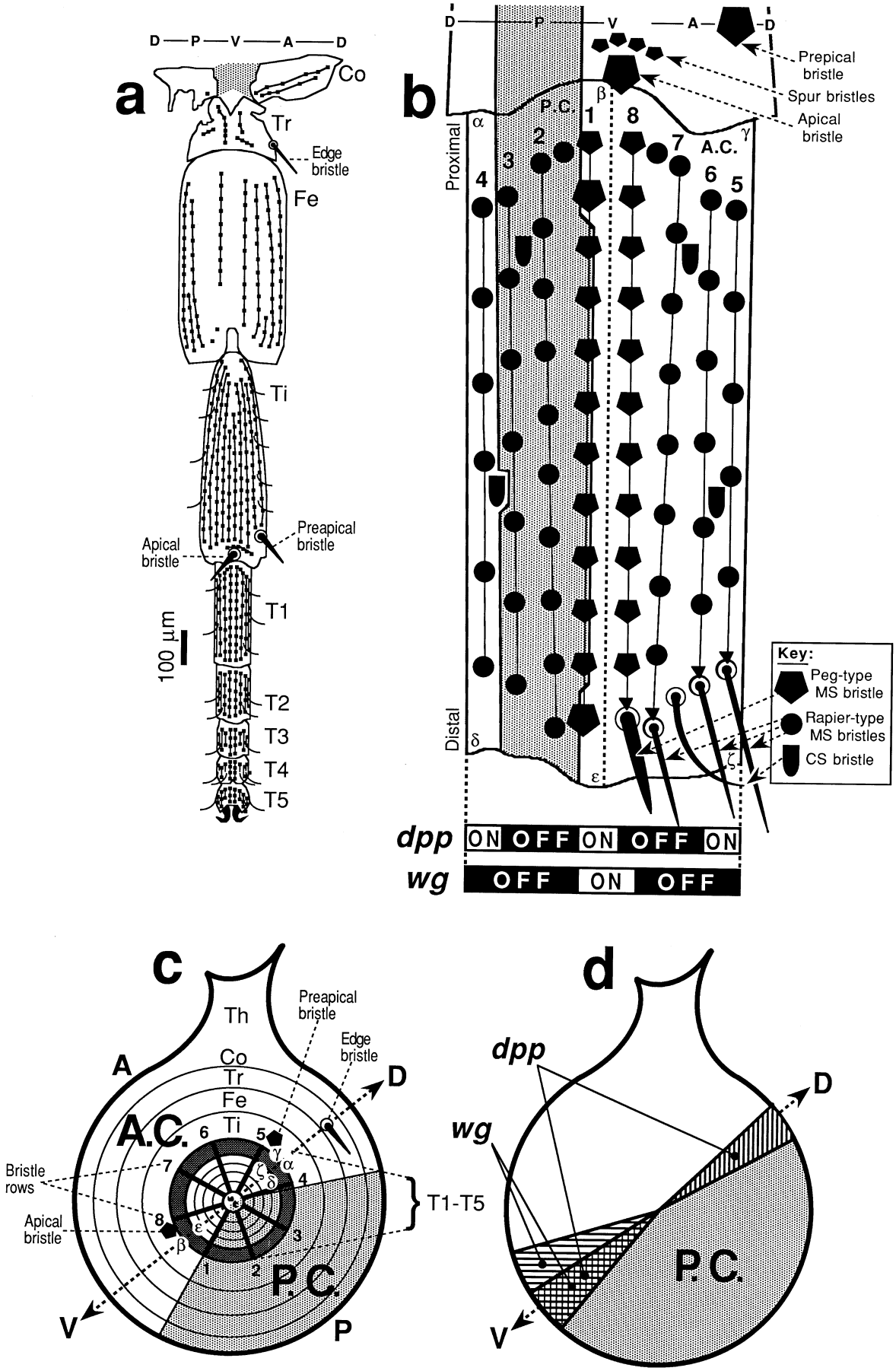

Legend to Fig. 1, see p 184

Materials and methods; Table 1), 72 basitarsi had *yellow* bristles in the A.C. (rows 4–8) and 81 basitarsi had *yellow* bristles in the P.C. (rows 2–3). Given that 1,000 legs were inspected in this cohort, the frequency of basitarsi with *yellow* bristles in both compartments should be about $0.072 \times 0.081 = 0.006 = 6$ cases among the 1,000 legs. Instead, we found 30 cases, 5 times the expected number. Likewise, there were 5 times the expected number of dual-compartment mosaicism in the second-instar control group: 121 out of 700 inspected basitarsi had marked bristles in the A.C. and 72 basitarsi had marked bristles in the P.C., yielding an expected frequency of $0.121 \times 0.072 = 0.012 = 12$ cases among 700 legs, but we found 55 such cases. Therefore, a leg that experiences a *FLP-FRT*-induced cross-over in one cell is apparently more likely than chance alone to experience a cross-over in other cells as well, so the multiple stripes are probably multiple clones (cf. Jiang and Struhl 1995; Li et al. 1995).

Given that our aim was to "knock out" *dpp* or *wg* gene function along the dorsal or ventral midlines where these genes are expressed (Fig. 1d), it was essential to determine whether clones would in fact "hit" those regions, so we measured how often *yellow* bristles occupy dorsal or ventral sites in *FLP-FRT* control flies. The basitarsus is well suited for mapping clones because its 8 longitudinal bristle rows are evenly spaced around the circumference (Fig. 1b), and the circa 10 bristles within each row are likewise evenly spaced, making this segment a cylindrical "display screen", each of whose 80 or so "pixels" (bristles) can be in one of two states – either wild-type (brown) or marked (yellow). Among the 137 mosaic basitarsi of the first-instar control group, the numbers of cases in which specific rows contained marked bristles were as follows, with rows listed in descending order of their frequency of "hits" (inclusion of marked bristles): row 2 (67 hits), 1 (45), 7 (41), 3 (35), 6 (28), 8 (27), 5 (24) and 4 (18). For the second-instar control group ($n = 145$ mosaic basitarsi), the data are: 2 (59), 7 (54), 8 (50), 6 (48), 1 (45), 5 (39), 4 (35) and 3 (35). These frequencies of hits were high enough in the dorsal (4 and 5) and ventral (1 and 8) rows that midline targets should often be overlapped by clones in the experimental series. In the first-instar control sample, 18 legs had 1

Fig. 1a–d Maps of wild-type leg anatomy, cell fates in the leg disc, and areas of gene expression. **a** Cuticular anatomy of a left second leg (after Grimshaw 1905; Hannah-Alava 1958; Held et al. 1986), diagrammed schematically. Mechanosensory bristles are symbolized by *squares* and chemosensory bristles by *curved lines*. Bristles belonging to the same row are *connected by straight lines*. The leg is drawn as if slit along its dorsal (*D*) midline, pried open, and flattened. The ventral (*V*) midline is centermost, with anterior (*A*) to the *right* and posterior (*P*) to the *left*. From the proximal to the distal end, the segments are: *Co* = coxa, *Tr* = trochanter, *Fe* = femur, *Ti* = tibia, *T1-T5* = the 5 tarsal segments. The *shaded area* of the coxa is membranous cuticle connecting the sclerotized front and back surfaces. The edge bristle of the trochanter lies on the dorsal midline. The preapical bristle of the tibia (so-named because it is just proximal to the segment's apex) likewise serves as a marker for the dorsal surface. Convenient markers for ventral identity are the tibial apical bristle and the peg-like basitarsal bristles in rows 1 and 8 (**b**). **b** "Standard" bristle pattern for the basitarsus (T1) of a left second leg (same orientation as in **a**). The numbering of the eight rows (*vertical lines*) obeys the nomenclature of Hannah-Alava (1958). [N.B. The nomenclature is backwards in Struhl and Basler (1993) and Diaz-Benjumea and Cohen (1994), where ventral rows are mislabelled as 4 and 5 and dorsal rows are mislabelled as 1 and 8.] The number of bristles in each row is the mean from a random sample of 40 control legs (non-heat-shocked F_1 male offspring from cross #1). Although row number is constant, the number of bristles per row varies from fly to fly. Symbols are explained in the key (*MS* mechanosensory, *CS* chemosensory), except for the *triangle*, which is a "bract" – a thickened trichome (non-innervated hair) that accompanies MS bristles on this segment (Hannah-Alava 1958). A few bristles are sketched in the *lower right*. They illustrate a dorsal-ventral gradient in bristle lengths found on both sides of the pattern. Similar gradients exist in the sizes of bristle intervals within the rows (ventral rows have closer bristles; Held 1990), endowing the segment with a bilateral symmetry accentuated by the symmetry of the CS bristle sites. On the distal tibia are two macrochaetes plus the distinctive array of peg-like ("spur") bristles that crowns the apical bristle, all of which are useful for dorsal versus ventral identification. (Other tibial bristles have been omitted). The peg-like bristles of the basitarsus also serve as ventral landmarks. The distalmost bristles in rows 1 and 8, as well as the second bristle in row 1 (which allows row 1 to be distinguished from row 8), are exceptionally large. The *shaded stripe* is the posterior cell-lineage compartment (*P.C.*, *A.C.* anterior compartment; Held 1979b). The bristles of row 1 can be embraced by clones from either compartment (Held 1979b; Lawrence et al. 1979). The relative frequency with which each bristle is affiliated with the P.C. is shown here by the extent to which its symbol resides in the shaded stripe. The true path of the A.C./P.C. boundary through the background epidermis is unknown. The basitarsus is about 70 cells long and 20 cells around (Held 1979a). Below the map are *bars* showing the approximate circumferential domains where the genes *dpp* and *wg* are transcribed (**d**). To aid the reader in comparing **b** and **c**, Greek letters (α-ζ) have been inscribed at the corners and midlines here and at identical sites in the diagram of the leg disc in **c**. **c** Fate map of the mature imaginal disc for a left leg (after Schubiger 1968, Girton 1982, and Held et al. 1994). The disc epithelium is a monolayer (Poodry and Schneiderman 1970). During metamorphosis, leg segments telescope outward from annuli in the disc (Fristrom and Fristrom 1975) – proximal segments from the periphery, distal segments from the center. The presumptive basitarsal area is *darkly shaded*. The posterior compartment is *lightly shaded*. Abbreviations and symbols are as in **a** and **b**. The stalk (*top*) which connects the disc with the larval epitheilum produces thoracic (*Th*) cuticle that is not part of the leg proper. Positions of bristle rows (*radial spokes*) and tibial macrochaetes are estimated relative to other mapped elements (Held et al. 1994; cf. Orenic et al. 1993). Claws are shown in the *center*, though their fate-mapped site is slightly more dorsal (Bodenstein 1941; Schubiger 1968), and they behave as dorsal elements in mutant phenotypes (Held et al. 1994). *A-P* and *D-V axes* refer to future axes of the leg, not to the orientation of the disc inside the larva. **d** Areas where the genes *dpp* (vertical hatching; Masucci et al. 1990; Raftery et al. 1991) and *wg* (horizontal hatching; Baker 1988a; Couso et al. 1993; Struhl and Basler 1993) are transcribed in the mature imaginal leg disc. Although *wg* is transcribed in the same sector throughout disc development (Couso et al. 1993), the dorsal sector of *dpp* transcription is not apparent in early third instar (Masucci et al. 1990). In mature discs, transcription of *dpp* is more intense dorsally than ventrally (Masucci et al. 1990). The *A.C./P.C. boundary* is offset by several cell diameters from the *D-V midline* (Steiner 1976; e.g. the edge bristle is in the A.C.). The amount of overlap between the *dpp* and *wg* areas is not precisely known, nor is it known whether the D-V midline bisects the *dpp* sectors (Held 1995).

(17 legs) or 2 (1 leg) *yellow* claws; in the second-instar sample, 32 legs had 1 (29 legs) or 2 (3 legs) *yellow* claws.

The *FLP-FRT* data reported below are for flies heat-shocked in the first instar. This stage was selected because the earlier the time of clone induction, the larger the eventual clone should be, and hence the greater the chance of eclipsing a large target region. By this logic, the γ-irradiations should also have been performed during the first instar so as to induce the largest possible clones. However, a pilot experiment using first-instar irradiations (cross #6) yielded too high a frequency of leg deformities (e.g. fused tarsal segments; cf. Postlethwait and Schneiderman 1973), so second-instar irradiations were used instead. Clone size was not compromised because a growth boost was provided by the *Minute* technique (see Materials and methods).

For control legs, the most frequently mosaic segment in every series was the femur or tibia, with mosaicism frequency decreasing proximally and distally (data not shown) in proportion to segment area. This correlation may be due to relatively uniform mitotic rates throughout the disc.

Effects of null clones along the proximal-distal axis of the leg

Table 1 summarizes the frequencies of mosaicism observed for various clonal genotypes. We used one *wg*-null genotype but three *dpp*-null genotypes. The reason for using so many different *dpp*-null genotypes was that each provided a different way of solving a peculiar problem with the *dpp* gene: *dpp* is one of the few genes in *D. melanogaster* to exhibit a haplo-insufficient phenotype (Ashburner 1989). An individual with only one functional *dpp* allele does not survive embryogenesis (Spencer et al. 1982; St. Johnston et al. 1990). The task, therefore, was to design heterozygotes whose non-functional *dpp* allele could be homozygosed without incurring the haplo-insufficient lethality. Posakony et al. (1991) solved this problem by constructing a heterozygote whose wild-type *dpp* alleles are both on a single chromosome arm, and we used such a fly stock (cross #6). In a second approach, we avoided the embryonic lethality of the *dpp*-null allele by using an "embryonic rescue" transposon inserted on the third chromosome (cross #5). Embryonic enhancers were intact in the transposon, but imaginal disc enhancers had been removed (Hursh et al. 1993). Finally (cross #2), we used a "Class V" (Spencer et al. 1982) *dpp* allele, dpp^{d12}, an inversion that disrupts the cis-regulation of *dpp* (St. Johnston et al. 1990). The intact dpp^{+} transcription unit of dpp^{d12} is expressed during embryogenesis but not, apparently, within the central part of the leg disc since the central domain of *Distal-less* gene expression is missing in dpp^{d12}/dpp^{d14} mutant larvae (Diaz-Benjumea et al. 1994: their Fig. 2). This absence implies that dpp^{d12} is effectively a null allele within the tarsus and distal tibia. To distinguish among these *dpp*-null genotypes, we designate them "$dpp^{null\text{-}M+}$" (for the "$Minute^{+}$" allele which enhances the clonal growth rate), "$dpp^{null\text{-}ER}$" (for "embryonic rescue" transposon) and "dpp^{d12}" respectively.

Frequencies of leg mosaicism ranged from 11 to 21% for *FLP-FRT* flies heat shocked during the first instar. Mosaicism frequencies for γ-rayed flies were an order of magnitude lower (2 to 3%), as expected (Steiner 1976). Regardless of the experimental genotype, less than 10% of the mosaic legs were abnormal. No abnormalities were found among control legs, except for rare (relatively trivial) bristle defects.

Three branched legs were recovered (not shown): two wg^{null} mosaics and one $dpp^{null\text{-}ER}$ mosaic. In both of the wg^{null} cases: (1) a right-handed side branch diverges from the ventral surface of the femur of a right leg (distal femur in one, proximal femur in the other), (2) the side branch contains more *yellow* bristles (circa 30–50% *yellow*, virtually all in the anterior compartment) than the main branch (circa 10%), and (3) the leg segments of the side branch are deformed (including tarsal segment fusions and, in one case, a spherical tibia whose bristle polarity is disturbed proximally), whereas the main branch is anatomically relatively normal (cf. Jiang and Struhl 1995). In the $dpp^{null\text{-}ER}$ branched leg, (1) a right-handed side branch diverges from the ventral (sic) surface of the trochanter of a right leg, (2) both branches contain high proportions of *yellow* bristles (up to 50% in proximal segments), and (3) both branches are abnormal: the side branch has a short femur and a deformed tibia whose bristle polarity is disturbed proximally, and the main branch terminates with the basitarsus and is tipped with necrotic tissue.

The most common leg abnormalities in each series involved the absence of pattern elements from the dorsal or ventral sides of specific leg segments, with or without the missing part being replaced by a duplicate version of the remaining part. When replacement does occur, the remnant and duplicate cuticular patterns are arranged as mirror images (see below). Segments midway along the leg (tibia, T1, T2) manifest such defects more frequently than proximal or distal segments. Among the 223 wg^{null} mosaic legs, 11 legs terminate with a segment other than T5. Four end with T1, 5 with T2, and 1 with T4. In each of the 11 cases, the terminal segment has: (1) a D/D phenotype, with *yellow* (wg^{null}) bristles on its ventral face, (2) nearly normal length (none are shorter than the basitarsus in Fig. 3g–i), though some taper distally, and (3) a D/D necrotic joint at its distal end. The necrosis is confined to the interiors of the duplicated sockets at the tip of the truncated leg. However, necrotic D/D joints were also found in legs which broke at this juncture after mounting, implying that the truncations are due to fragility of the D/D joint itself. Truncations were more rare (less than 2% of mosaic legs) in the other mutant genotypes ($dpp^{null\text{-}ER}$, dpp^{d12}, and dpp^{d12} wg^{null}; none in the controls). Aside from deficiencies, duplications and truncations, the only other noteworthy abnormalities were infrequent deformities (including shortening) of mosaic fe-

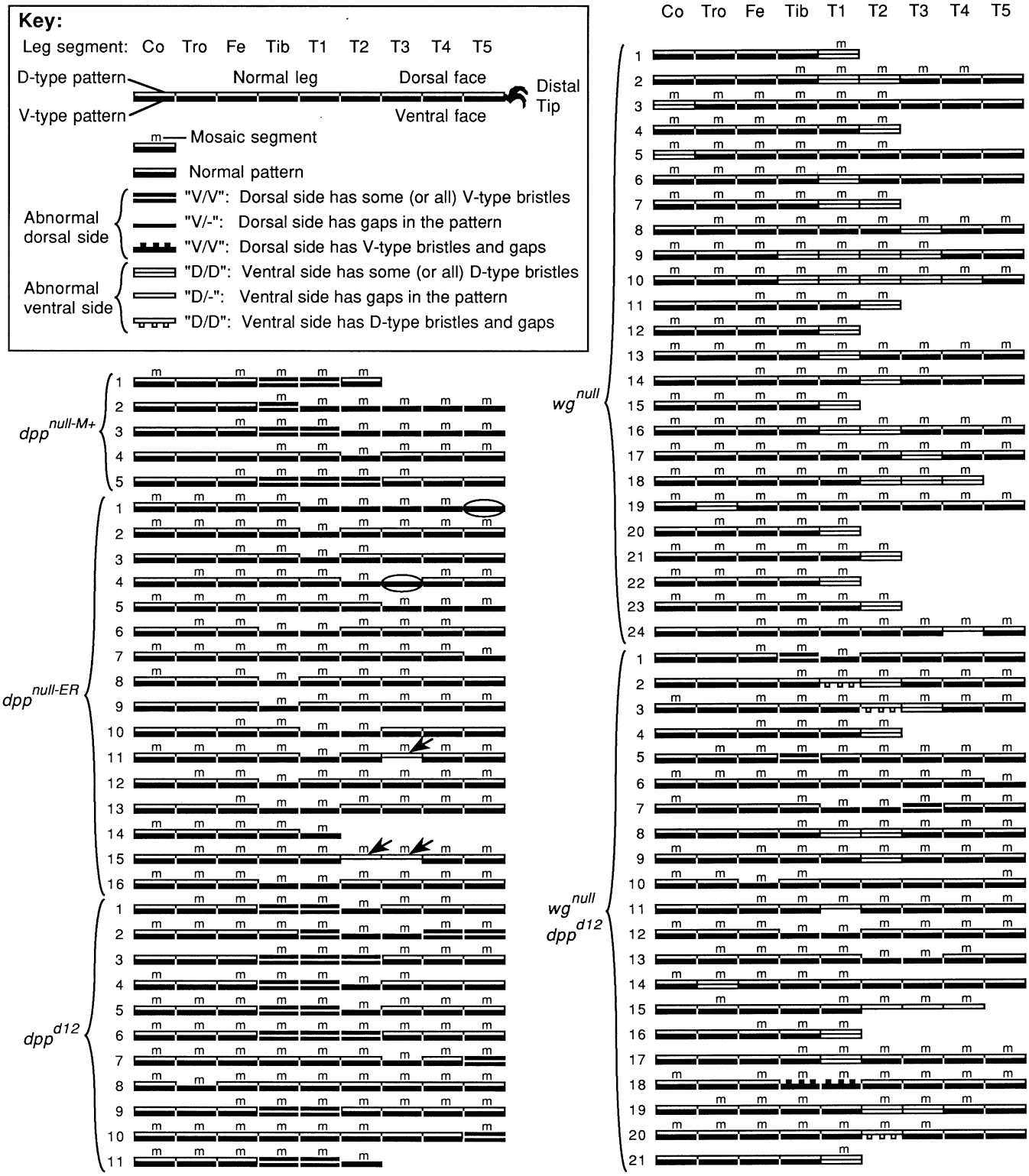

Fig. 2 Mosaic legs which contain a dorsally or ventrally abnormal pattern in at least one leg segment. Legs are grouped according to clone genotype (*listed at the left of each bracketed group*). Symbols are explained in the key. Note the predominance of V/V segments among *dpp*-null mosaic legs versus the high frequency of D/D segments among *wg*-null mosaic legs. *Ovals* encircle abnormal segments that contained no marked bristles. *Arrowheads* indicate segments in the *dpp*-null series which showed ventral, rather than dorsal abnormalities. Leg truncations were most common in the wg^{null} series (see text)

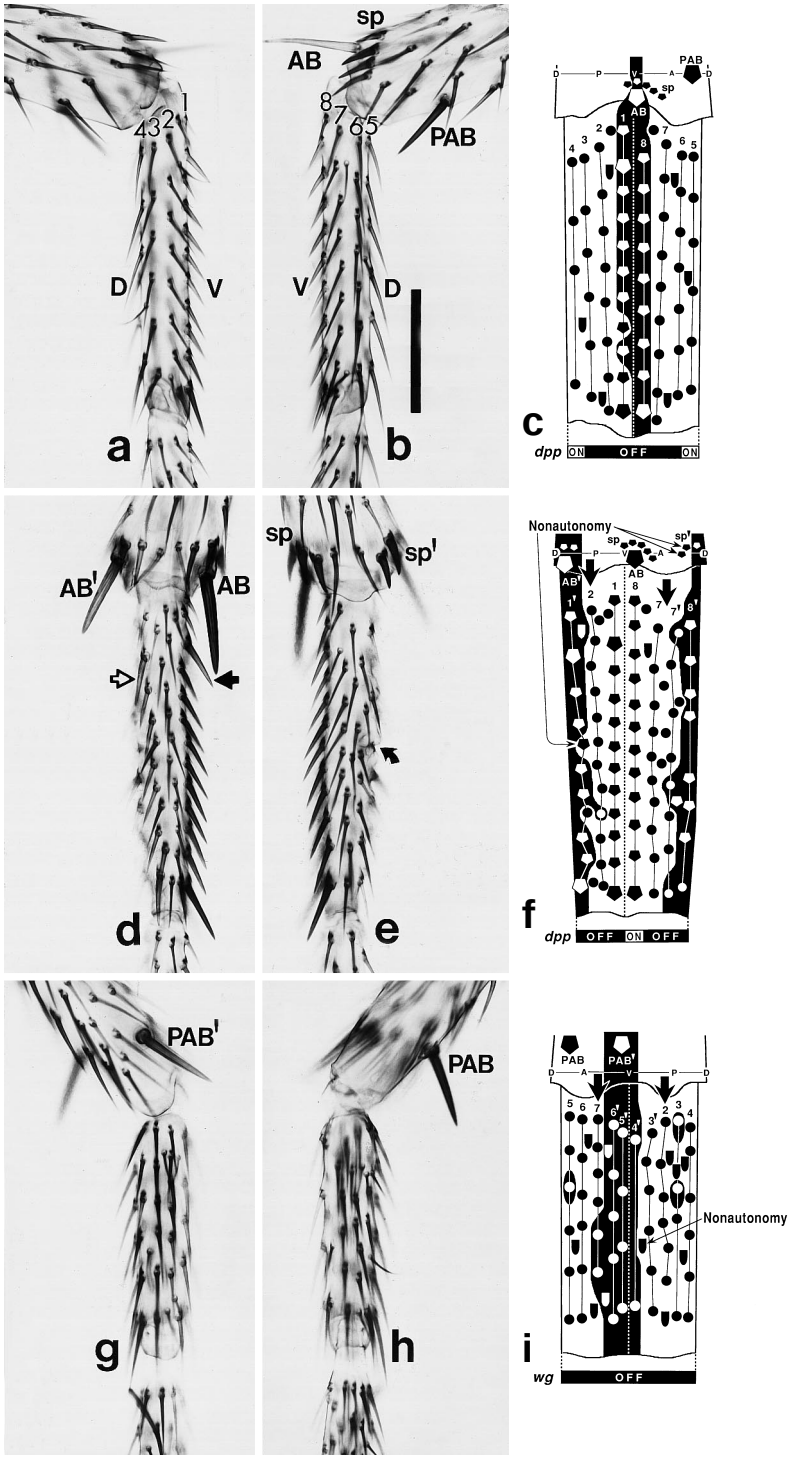

Fig. 3a–i Mosaic basitarsi, including extreme cases of Janus pattern duplications [*AB* apical bristle, *PAB* preapical bristle, *sp* spur bristles, *D* dorsal, *V* ventral, *A* anterior, *P* posterior, *Prime marks* extra ectopic bristles, *Numbers* designate bristle rows (cf. Fig. 1b); in schematic diagrams: *pentagons* peg-shaped bristles, *circles* rapier-shaped bristles, *bullets* curved chemosensory bristles, *unfilled symbols* genetically marked (*dpp*-null or *wg*-null) bristles]. **a-c** Basitarsus of the left second leg from a mosaic fly whose marked (*straw*) bristles are $dpp^{null\text{-}M+}$ (cross #6; see Materials and methods). **a** Posterior face. "*D*" and "*V*" denote the dorsal and ventral edges, and paired pictures in the other panels (**d** and **e**; **g** and **h**) are oriented likewise (i.e. ventral sides facing each other). **b** Anterior face. Note that the apical bristle (*AB*) on the tibia is lighter in color than the preapical bristle (*PAB*), which is indicative of its mutant genotype. The apical bristle is crowned with an arc-shaped row of spur bristles (*sp*, *Bar* 100 μm). Magnifications are the same for all panels in this figure. **c** Schematic map. *Unfilled symbols* denote *straw*, $dpp^{null\text{-}M+}$ bristles. Here, (and in **f** and **i**) a *black background* has been drawn around mutant bristles as a visual aid, though the actual path of the boundary in the background epidermis is unknown, and the *dashed line* marks the ventral midline. Below the map is a *bar* indicating the presumed state of the *dpp* gene around the circumference of this segment. Because the ventral face (rows 1 and 8) is virtually all dpp^{null}, there should be no ▶

dpp expression there. Despite this absence of ventral expression, the pattern appears normal. There are two odd, but trivial, features: row 8 lacks its most proximal bristle, and row 4 has few bristles. **d–f** Basitarsus of the left second leg from a mosaic fly whose genetically marked (*yellow*) bristles are dpp^{d12} (cross #2; dpp^{d12} leg #1 in Fig. 2). **d** Posterior face. Note that while the apical bristle (*AB*) is present at its normal site, the preapical bristle has been replaced with a mutant apical bristle (*AB′*), which makes the distal tibia symmetric. The basitarsus also has a double-ventral ("V/V") pattern, with an ectopic (mostly mutant) row 1 located dorsally in mirror image to the normal row 1 on the ventral side. There are peg-shaped bristles in both rows. The *solid* and *hollow arrows* point to enlarged penultimate bristles characteristic of row 1. **e** Anterior face. The mirror symmetry is also evident on this side of the tibia, where an extra group of spur bristles (*sp′*) lies dorsally. Note that two of these bristles have wild-type pigmentation, indicating that wild-type cells were recruited nonautonomously to form part of the abnormal pattern territory. The normal row 8 is visible along the *left edge*. An ectopic (mutant) row 8 is out of focus along the *right edge*. The *curved arrow* points to a sclerotized invagination that resembles a tarsal joint. Similar invaginations were observed in comparable locations of other V/V basitarsi, and they are associated (as here, though not in focus) with disturbances of bristle and/or bristle-bract polarity nearby. **f** Schematic map. *Unfilled symbols* denote *yellow*, dpp^{d12} bristles. Rows 3, 4, 5, and 6 are missing, and in their place are extra copies of rows 1, 8 and 7 (*1′*, *8′*, *7′*). *Thick arrowheads* indicate the V/V plane of symmetry. The dorsal-to-ventral transformation is imperfect because one bristle (*circle symbol*) in each of the rows 1′ and 8′ is not peg-shaped. (Bristle alignment and spacing are also abnormal.) Note that one of the peg-type bristles in row 1′ (*arrow*) is wild-type, another case of nonautonomy like the wild-type ectopic spur bristles on the dorsal tibia. Below the map is a *bar* indicating that this dorsal mutant clone should have eliminated all *dpp* expression along the dorsal midline, an absence which has evidently triggered this V/V phenotype. **g–i** Basitarsus of the right (*sic*) second leg from a mosaic fly whose genetically marked (*yellow*) bristles are wg^{null} (cross #3; wg^{null} leg #10 in **Fig. 2**). **g** Anterior face. Note the absence of peg-shaped (ventral-type) bristles from the ventral side (*right edge*) of the basitarsus. In their place are genetically marked rapier-shaped bristles that are typical of the dorsal side, thus endowing the segment with a double-dorsal (D/D) symmetry. Similarly, the ventral surface of the tibia now displays a mutant preapical bristle (*PAB′*) typical of the dorsal surface, and spur bristles are missing. The basitarsus is shorter and wider than normal. (A stray bristle overlaps the second tarsal segment.) **h** Posterior face. Here too, all peg-type bristles are missing and replaced by rapier-type bristles. **i** Schematic map. *Unfilled symbols* denote *yellow*, wg^{null} bristles. Rows 1 and 8 are absent. In their place are extra copies of rows 6, 5, and 4 (*6′*, *5′*, *4′*), and an ectopic preapical bristle (*PAB′*) resides where the apical bristle should be. *Thick arrowheads* indicate the D/D plane of symmetry. The ventral stripe of mutant cells has apparently eliminated all *wg* expression (see *bar* below the map), which has resulted in this D/D phenotype. There are three scattered *yellow* bristles besides those in the ventral stripe. A definitive sign of the D/D transformation is the presence of chemosensory bristles on the ventral surface, one of which (*arrow*) is wild-type, indicating that this wild type cell has been nonautonomously recruited into the abnormal pattern

murs and tibiae from the *dpp*-null series (< 3% of mosaic legs).

Among *dpp*-null mosaic legs, a single claw (anterior or posterior) was often *yellow*: 26/213 $dpp^{null\text{-}ER}$ mosaic legs had one marked claw; as did 20/207 dpp^{d12} mosaic legs; but only 2/73 $dpp^{null\text{-}M^+}$ mosaic legs had a marked claw. In none of these series were both claws marked. (Nonautonomy of claw formation was also found with the heteroallelic *dpp* genotype dpp^{d6}/dpp^{d14}; Spencer 1984). Rarely, legs were missing one claw (3/213 $dpp^{null\text{-}ER}$ mosaic legs; 0/207 dpp^{d12} mosaic legs) or both claws (5/213 $dpp^{null\text{-}ER}$ mosaic legs; 4/207 dpp^{d12} mosaic legs). In the γ-ray series, missing claws were common even in controls, probably due to irradiation compounded by a sensitive genotype (cf. Haynie and Bryant 1977; Lawrence et al. 1986). For all data on claw mosaicism or absence reported here, the samples exclude truncated legs. For the wg^{null} mosaics, there were cases where one or both claws were *yellow* (14/212 wg^{null} mosaic legs had one marked claw; in 1/212 leg both claws were marked), but there were no instances of missing or duplicated claws. In the double-mutant dpp^{d12} wg^{null} series, there were 18/221 cases of a single *yellow* claw (no cases of both claws marked), with 4/221 legs missing both claws.

Effects of null clones along the dorsal-ventral axis of the leg

The main focus of this investigation is the dorsal-ventral axis of the leg and the relative roles played by *dpp* and *wg* in cuticular patterning along this axis. Table 1 lists the types of abnormalities observed along the axis, and Fig. 2 schematically depicts all legs that exhibited such abnormalities. Since individual legs never manifested abnormalites in all of their segments, we statistically analyzed leg segments rather than whole legs. The broadest two categories of leg segment abnormalities are: (1) segments which are dorsally abnormal or (2) segments which are ventrally abnormal. Pooling all of the data from the three different *dpp*-null genotypes, there were 73 cases of a leg segment being dorsally abnormal versus only 3 cases of a leg segment being ventrally abnormal (Table 1). A reciprocal imbalance was observed with *wg*-null mosaic legs: no dorsally abnormal leg segments were found versus 36 leg segments which are ventrally abnormal. In mosaic legs which carry doubly mutant dpp^{d12} wg^{null} clones, the frequencies of dorsally abnormal (14 cases) and ventrally abnormal (19 cases) leg segments are roughly equal.

The failure to find ventrally defective leg segments in the *dpp*-null mosaics is not due to a paucity of clones in the ventral region. The distribution of clonal "hits" around the basitarsal circumference in the three *dpp*-null experiments was comparable to control frequencies cited above. Thus, the numbers of basitarsi in which the ventral rows 1, 2, 7 and 8 were mosaic were: 18, 16, 18 and 10 hits in the $dpp^{null\text{-}M^+}$ series (n = 51 mosaic basitarsi), 53, 62, 32 and 27 hits in the $dpp^{null\text{-}ER}$ series (n = 147 mosaic basitarsi), and 54, 61, 24 and 13 hits in the dpp^{d12} series (n = 134 mosaic basitarsi).

Within each broad category of dorsal or ventral abnormality, there are two classes of phenotypes: leg segments which are merely deficient for the pattern elements of the abnormal side ("V/-" or "D/-") and leg segments whose missing elements are replaced by extra copies of pattern elements that are normally (in wild-type flies) only found on the opposite side ("V/V" or

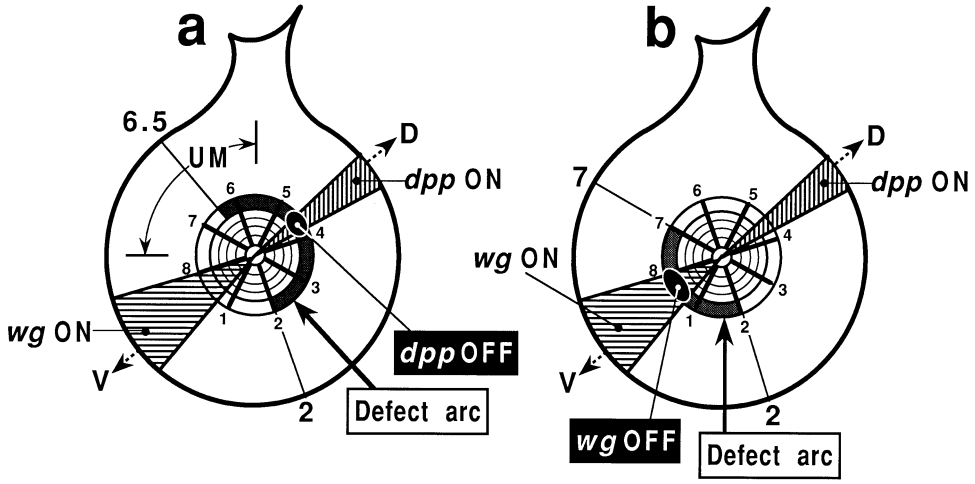

Fig. 4a, b Projection of leg abnormalites from **Fig. 3** onto a fate map of the leg imaginal disc, augmented to show the expression domains of *dpp* and *wg*. (See Fig. 1 for uncertainties in the map.) "*ON*" denotes that a gene is functional, not merely transcribed. Given that so few defects were found for ventral *dpp*-null clones, the ventral sector of *dpp* transcription is unlikely to be functional, so it has not been drawn. **a** Effects of a dorsally located *dpp*-null clone (abstractly represented as a *black oval*), as seen on the basitarsus in **Fig. 3d–f**. Other segments have been ignored in this schematic. The consequence of turning *dpp* OFF at this site is the loss of bristle rows 3, 4, 5, and 6 and their replacement with copies of rows 7, 8, and 1. Because the resulting mirror-image pattern contains two copies of row 7 (**Fig. 3f**), the symmetry plane (*thin line*) must reside just dorsal to row 7 ("*6.5*" denotes the area between rows 6 and 7), but it must run along row 2 since only a single row 2 is present. Thus, the affected domain of the basitarsal circumference describes a "*defect arc*" as shown. "*UM*" is the upper medial quadrant of the disc, which is presumed to contain most of the circumferential positional values of the disc (French et al. 1976). The V/V phenotype might therefore be due to removal of more than half the angular positional values in the defect arc, followed by intercalary regulation as dictated by the rules of the Polar Coordinate Model (see text). **b** Effects of a ventrally located *wg*-null clone (*black oval*), as observed on the basitarsus depicted in **Fig. 3g–i**. The consequence of turning *wg* OFF at this site is the loss of bristle rows 1 and 8 and their replacement with copies of rows 3, 4, 5, and 6. Because the resulting mirror-image pattern contains single copies of rows 2 and 7, the symmetry plane (*thin line*) must run along both of these rows. Hence, the defect arc for the *wg*-null clone (**b**) is almost exactly complementary to the defect arc for the *dpp*-null clone (**a**). The V-to-D transformation caused by the *wg*-null clone might be due to a derepression of the *dpp* gene within its normally nonfunctional ventral transcription sector (see text)

"D/D"). The *dpp*-null genotypes produced more deficient than duplication-deficient phenotypes (44 V/- versus 29 V/V), whereas nearly all of the wg^{null} mosaics manifested duplication-deficient phenotypes (35 D/D versus 1 D/-). Doubly mutant dpp^{d12} wg^{null} clones produced both kinds of phenotypes (5 V/V versus 9 V/-, and 15 D/D versus 4 D/-) and 5 duplication-deficient leg segments showed gaps in the duplicate pattern – i.e. bare areas of smooth cuticle where bristles would normally arise (Fig. 2).

In the most extreme cases of V/V and D/D duplications (Fig. 3), the duplicate patterns manifest a striking mirror-image symmetry about the plane separating them. Interestingly, the location of the tarsal mirror-symmetry plane is virtually the same in the V/V and D/D phenotypes. Dividing the disc into a ventral wedge and a complementary dorsal piece, the mirror plane is roughly coincident with bristle rows 2 and 7 (Fig. 4). Wild-type bristles are occasionally found to nonautonomously participate in the duplicate (ventral or dorsal) pattern. For example, two of the spur bristles associated with the ectopic (mutant) apical bristle in a V/V tibia from the dpp^{d12} mosaic series are wild-type (Fig. 3d–f). When the distal end of a tarsal segment's bristle pattern manifests a V/V phenotype, it typically lacks the internal structures of the joint at that end, whereas if it has a D/D phenotype there are usually two sockets and condyles in mirror image.

Discussion

Only the dorsal half of the dpp transcription stripe is functional

Campbell et al. (1993) proposed that the center of the leg disc is a "distal organizer" for the leg because this is the only place where the ventral sector of *wg* expression and the dorsal sector of *dpp* expression intersect. However, *dpp* is also transcribed in a ventral sector (Fig. 1d), which is problematic for the model. Most authors have assumed that the ventral sector of *dpp* transcription is nonfunctional (reviewed in Blair 1995b; Campbell and Tomlinson 1995; Held 1995), but until now this speculation has not been directly tested. Here we report that incapacitation of the *dpp* gene in the ventral region has virtually no effect, thus validating the assumption. Despite "hitting" the ventral bristle rows 1, 2, 7 and 8 with *dpp*-null clones a total of 125, 139, 74 and 50 times respectively, no ventrally defective basitarsi were recovered. Only three cases of ventrally defective leg segments were observed in the *dpp*-null series (Fig. 2). In contrast, 73 leg segments were dorsally defective (Table 1, Fig. 2). This ability of *dpp*-null clones to induce dorsal but not ventral defects implies that only the dorsal half of the

dpp stripe is functional in pattern formation. In contrast to our findings for the leg, a similar analysis for the wing showed that *dpp* is needed along its entire (ventral and dorsal) stripe of expression there (Posakony et al. 1991). Affirming this difference in the leg versus the wing, Morimura et al. (1996) reported stronger effects on leg than on wing development when *dpp* protein levels are artificially increased in both discs (by activating a UAS-*dpp* transgene with a *dpp*-GAL4 driver). Most of the defects that they observed are on the ventral side of the leg, suggesting that *dpp* function is normally suppressed there, but that this suppression can be overridden by *dpp* overexpression.

If the disc center is a key reference point for proximal-distal patterning as proposed by Campbell et al. (1993) and presaged by Meinhardt (1980, 1983), then it might be possible to inactivate this "bull's-eye" by hitting it with a *dpp*- or *wg*-null clone. Rare leg truncations were observed in all five experimental series, most often in the wg^{null} series where 11 (5%) out of 223 mosaic legs ended in T1-T4 (Fig. 2; cf. Couso et al. 1993). However, these are not the kinds of truncations expected for a "dead" organizer. They appear to be artifacts of leg breakage at necrotic D/D joints (cf. Held et al. 1994). None of the truncations resembles those caused by *Distal-less* (a.k.a. *Brista*) mutations (Cohen and Jürgens 1989; Held et al. 1994) – i.e. legs that end in the middle of a leg segment. Nevertheless, this negative result may still be consistent with the organizer hypothesis. The organizer might reside not in the claws but in the nearby cluster of nondividing cells discovered by Graves and Schubiger (1982). "Knock-outs" might thus be averted since this site would be immune to mitotic crossing over or invasion from nearby clones.

Effects of null clones do not spread along the proximal-distal axis

The effects of null clones are generally confined to the segments where they are located. Only two legs were found where abnormal segments were nonmosaic (Fig. 2). Although these cases may indicate trans-segmental effects, mutant cells might have been present in the affected segments long enough to disrupt patterning before vanishing. With possible rare exceptions, therefore, *dpp*- and *wg*-null clones only affect patterning within their own segment. Since each segment develops as an annulus in the disc (Fig. 1c), this conclusion seems to rule out a Cartesian coordinate system wherein *dpp* and *wg* signals travel in lines perpendicular to the sectors where they are expressed, because such lines cross segment boundaries (Winfree 1980; Kauffman and Ling 1981; Meinhardt 1983; Russell 1985; Gelbart 1989; Papageorgiou 1989; Held 1995).

Not only can the pattern of a single segment be clonally modified without any disturbances in other segments, but the various parts of a single bristle row can be transformed independently of one another. For example, one basitarsus (leg # 2) in the dpp^{d12} wg^{null} series (Fig. 2, details not shown) has 12 bristles in the row 8 area: the proximal 9 (8 y^+, 1 *y*) are peg-shaped ("V-type"), the distal 3 (all *y*) are rapier-shaped ("D-type" as in row 4 or 5), and the V- and D-type bristles are closely versus widely spaced as they would be in situ (Fig. 1b). This balkanization of the pattern, which is the general rule (though transitions are not always so abrupt), implies that even sub-segmental sections of the proximal-distal axis are under separate control. This conclusion is bolstered by the ability of different subsets of the 3′ ensemble of *dpp* enhancers to drive *dpp* expression in different parts of its transcription stripe (Massuci et al. 1990; Blackman et al. 1991; Sanicola et al. 1995). Thus, annuli that are only a few cells wide may be patterned independently.

Effects of null clones are confined to sectors of the circumference

The most frequent type of abnormality caused by null clones (seen in 84 leg segments: Table 1, Fig. 2) is the replacement of D-type bristles with V-type bristles (*dpp*-null clones) or vice versa (*wg*-null clones). In the most extreme transformations, segments have two nearly identical half-patterns arranged as "Janus" mirror-images (Fig. 3). Comparable V/V and D/D phenotypes were previously reported for *dpp* and *wg* hypomorphs (Spencer et al. 1982; Baker 1988b; Bryant 1988; Peifer et al. 1991, Couso et al. 1993; Held et al. 1994). In both the mosaics analyzed here and the hypomorphs studied earlier, the plane of V/V symmetry is virtually identical to the plane of D/D symmetry (Fig. 4). In the disc, this plane describes two radii (roughly along bristle rows 2 and 7) which define a large dorsal sector (~225°) and a small ventral sector (~135°). The pattern defects caused by *dpp*-null clones are mostly confined (73/76 segments) to the dorsal domain and those caused by *wg*-null clones are restricted (36/36 segments) to the ventral domain. The condyles and sockets of the tarsal joints also obey this rule. These dorsal structures (Held et al. 1986, 1994) are typically missing in V/V and V/- segments and duplicated in D/D segments. The significance of the complementary dorsal and ventral domains is unknown (Held 1995).

The second-most common abnormality caused by null clones is elimination of dorsal or ventral structures without any replacement (shown by 61 leg segments). This phenotype was observed 20 times more often (44 segments out of 493 legs) with *dpp* mosaics than with *wg* mosaics (1 segment out of 223 mosaic legs). To explain why *dpp* hypomorphs commonly show V/- phenotypes whereas *wg* hypomorphs do not not show D/- phenotypes, it has been argued (Held et al. 1994) that the V/V phenotype must be reached via a V/- stage, whereas the D/D phenotype may have no comparable D/- transitional state. Depending upon when a *dpp*-null clone initiaties a duplication, the duplication process may get "caught in the act" (in its V/- stage) at metamorphosis.

How do the V/V and D/D phenotypes arise? The Polar Coordinate Model explains such duplications by assuming a removal of more than half of the angular coordinates, followed by juxtaposition of flanking cells and intercalation by the shortest route (French et al. 1976). Mutations in many genes produce cuticular duplications (Bryant 1978; Bryant and Girton 1980; James and Bryant 1981) and cell death is often the cause of tissue loss. Extensive apoptosis has been observed in *dpp* mutant leg discs (Bryant 1988), supporting the idea that the V/- state is created in this way, whereas cell death is not associated with *wg* phenotypes (Morata and Lawrence 1977; James and Bryant 1981; Williams et al. 1993). Perhaps the *dpp* protein is an essential growth factor for cell survival in the dorsal domain (Cross and Dexter 1991; Collins et al. 1994). Since most of the angular coordinates are crowded into the upper medial quadrant (Schubiger 1971; French et al. 1976; French and Daniels 1994; Fig. 4a), removal of the *dpp* domain could delete more than half of all the angular coordinates. Nevertheless, it is hard to imagine how a hole created by a 225° defect arc could heal so as to juxtapose cells from opposite ends of the arc (cf. Girton 1981, 1982; Girton and Berns 1982; Girton and Kumor 1985).

To explain the origin of D/D leg phenotypes in *wg* hypomorphs, it has been conjectured that: (1) *wg* normally suppresses ventral *dpp* function (Held et al. 1994; cf. Jiang and Struhl 1995), (2) reduction of *wg* levels allows *dpp* to up-regulate ventrally, and (3) this up-regulation leads to a mirror-symmetric D/D pattern because *dpp* protein functions as a dorsalizing morphogen. The ability of *dpp* overexpression to override *wg* ventrally (Morimura et al. 1996) supports this idea and suggests that *dpp* and *wg* are mutually antagonistic (cf. Penton and Hoffmann 1996). If a *wg*-null clone overlaps the ventral sector, then according to this logic, *dpp* could produce functional protein there, and a D/D pattern would develop in the affected annulus (Fig. 4).

Given that *dpp* and *wg* are members of growth factor families (*Wnt* and TGF-β respectively; Nusse and Varmus 1992; Padgett et al. 1987), and that both genes produce diffusible proteins in the embryo (Panganiban et al. 1990; González et al. 1991), it seems likely that they govern the cells within their respective (225° and 135°) domains by means of diffusion. However, no *wg* protein has been detected at distances greater than a few cell diameters outside the *wg* transcription sector (Wilder and Perrimon 1995), and the diffusion range of functional *dpp* protein is unknown because suitable antibodies to the carboxy (ligand) end of the protein are not yet available (M. Hoffmann, personal communication). It remains to be seen how any molecule can travel in an arc-shaped path over distances of tens or hundreds of cells. Many genes are expressed in annuli within the leg disc (Bryant 1993; Chang et al. 1993; Mardon et al. 1994; Goto et al. 1995; Villano and Katz 1995), but it is unclear how they might channel a graded *dpp* signal. The evidence for a *dpp* morphogen gradient in the wing disc is stronger (Nellen et al. 1996), and in that case the signal evidently diffuses normally, resulting in a linear rather than a curved gradient (cf. Held 1995).

No single bristle on any segment behaves like a trigger for pattern alteration in mosaic legs. Thus, *dpp*-null clones frequently include the dorsally located trochanteral edge bristle, the tibial pre-apical bristle or many bristles in rows 4 and 5 on the basitarsus without affecting the pattern, and *wg*-null clones can include the apical bristle or basitarsal peg bristles without any disturbance. A sufficient area of overlap with the dorsal (*dpp*-null clones) or ventral (*wg*-null clones) midline seems critical for instigating pattern reorganization. On the basitarsus, the threshold clone width seems to be about two bristle rows (~12% of the circumference), corresponding to roughly a 45° sector in the disc. The rarity of leg duplications in *wg*-null mosaics (only 2 branched legs and 24 internally duplicated legs out of 2000 legs examined here; cf. Jiang and Struhl 1995) may be due to a nontrivial target size and might explain why no abnormal legs were obtained in an earlier mosaic study that used a lethal *wg* allele (Baker 1988a; cf. Morata and Lawrence 1977).

Mosaics for signal-transduction genes show similar defects

Several genes in the *wg*-signaling pathway have been studied in genetic mosaics (Klingensmith and Nusse 1994; Siegfried and Perrimon 1994). One is *shaggy/zeste-white 3* (*sgg*), which encodes a protein kinase (Bourouis et al. 1990; Siegfried et al. 1990; Ruel et al. 1993). When a hypomorphic *sgg* allele was homozygosed in leg cells during the second instar, V-type bristles were found in the clones regardless of their circumferential location (Wilder and Perrimon 1995). The bristles are always appropriate for their proximodistal level of the segment – a result which affirms the separability of cellular identities along the dorsal-ventral and proximal-distal axes. When located ventrally, the *sgg* mutant clones integrate into the pattern, whereas dorsal clones often round up as islands or pinch off internally as invaginations or vesicles (L. Held, unpublished observations). On the basitarsus, *sgg* mutant clones exclusively produce peg-type (row-1 and row-8 type) bristles regardless of which bristle row they occupy (Wilder and Perrimon 1995). Since receipt of the *wg* signal in wild-type flies is thought to be transduced by inactivating the *sgg* kinase (Klingensmith and Nusse 1994), a partial-loss-of-function *sgg* allele like this one (Ruel et al. 1993) should reveal how "competent" cells respond to the *wg* signal. The implication is that *wg* only specifies row 1 and 8 identities. However, our results show that the "sphere of influence" of *wg* extends to rows 2 and 7 (Fig. 4), whose bristles are distinct from those in rows 1 and 8.

Another component of the *wg*-signaling pathway (downstream of *sgg*) is a homolog of the adherens junction protein β-catenin encoded by *armadillo* (*arm*; Peifer and Wieschaus 1990; Peifer et al. 1994a,b). When

first-instar larvae were γ-irradiated to induce cell clones homozygous for mutant alleles of *arm*, virtually no clones were recovered in the ventral half of the disc (Peifer et al. 1991), but they evidently lived long enough to alter leg development because the irradiated individuals manifested D/D pattern duplication-deficiencies. The boundary between the duplicated regions is the same as the symmetry plane in our D/D *wg*-null mosaic legs (Fig. 4).

Double-dorsal Janus leg phenotypes are caused by mutations in still another gene involved in *wg*-signal transduction (upstream of *sgg*)-*dishevelled* (*dsh*). The *dsh* gene encodes a possible cell junction protein (Klingensmith et al. 1994; Yanagawa et al. 1995). Mosaics for a lethal *dsh* allele show defects (bifurcations) in a ventral region bounded by tarsal bristle rows 2 and 6 (Klingensmith et al. 1994; Theisen et al. 1994), which roughly matches our *wg* domain (Fig. 4).

In the *dpp* signaling pathway the only gene analyzed so far in mosaic legs is *punt*, which encodes the Type-II *dpp* receptor. Clones that are mutant for a hypomorphic *punt* allele blend normally into the background pattern everywhere except dorsally (in segments distal to the femur): dorsal clones cause V/- and V/V defects like those reported here (Penton and Hoffmann 1996).

Acknowledgements *FRT*-insert "starter" stocks came from the Bloomington *Drosophila* Stock Center. Norbert Perrimon provided the *FLP*-bearing *MKRS* balancer, Nicholas Baker gave us a wg^{CX4} stock, and Vern Twombly furnished all *dpp* stocks, except for the dpp^{d12} allele which came from Rosalynn Miltenberger. Clint Hardee and Angelina Fusco helped with pupal collections and fly sorting. Constructive comments on the manuscript were kindly provided by David Sudderth, John Fondon and anonymous reviewers. This investigation was supported by a grant from the Howard Hughes Medical Institute through the Undergraduate Biological Sciences Education Program.

References

Ashburner M (1989) *Drosophila:* A laboratory handbook. Cold Spring Harbor Press, New York

Baker NE (1987) Molecular cloning of sequences from *wingless*, a segment polarity gene in *Drosophila*: the spatial distribution of a transcript in embryos. EMBO J 6: 1765–1773

Baker NE (1988a) Embryonic and imaginal requirements for *wingless*, a segment-polarity gene in *Drosophila*. Dev Biol 125: 96–108

Baker NE (1988b) Transcription of the segment-polarity gene *wingless* in the imaginal discs of *Drosophila*, and the phenotype of a pupal-lethal *wg* mutation. Development 102: 489–497

Blackman RK, Sanicola M, Raftery LA, Gillevet T, Gelbart WM (1991) An extensive 3′ *cis*-regulatory region directs the imaginal disk expression of *decapentaplegic*, a member of the TGF-β family in *Drosophila*. Development 111: 657–665

Blair SS (1995a) Compartments and appendage development in *Drosophila*. BioEssays 17: 299–309

Blair SS (1995b) Hedgehog digs up an old friend. Nature 373: 656–657

Bodenstein D (1941) Investigations on the problem of metamorphosis. VIII. Studies on leg determination in insects. J Exp Zool 87: 31–53

Bourouis M, Moore P, Ruel L, Grau Y, Heitzler P, Simpson P (1990) An early embryonic product of the gene *shaggy* encodes a serine/threonine protein kinase related to the CDC28/cdc2$^+$ subfamily. EMBO J 9: 2877–2884

Bryant PJ (1978) Pattern formation in imaginal discs. In: Ashburner M, Wright TRF (eds) The genetics and biology of *Drosophila*, Vol. 2c. Academic Press, New York, pp 229–335

Bryant PJ (1988) Localized cell death caused by mutations in a *Drosophila* gene coding for a transforming growth factor-β homolog. Dev Biol 128: 386–395

Bryant PJ (1993) The Polar Coordinate Model goes molecular. Science 259: 471–472

Bryant PJ, Girton JR (1980) Genetics of pattern formation. In: Siddigi et al. (eds) Development and neurobiology of *Drosophila*. Plenum, New York, pp 109–127

Bryant PJ, Schneiderman HA (1969) Cell lineage, growth, and determination in the imaginal leg discs of *Drosophila melanogaster*. Dev Biol 20: 263–290

Campbell G, Tomlinson A (1995) Initiation of the proximodistal axis in insect legs. Development 121: 619–628

Campbell G, Weaver T, Tomlinson A (1993) Axis specification in the developing *Drosophila* appendage: the role of *wingless*, *decapentaplegic*, and the homeobox gene *aristaless*. Cell 74: 1113–1123

Chang Z, Price BD, Bockheim S, Boedigheimer MJ, Smith R, Laughon A (1993) Molecular and genetic characterization of the *Drosophila tartan* gene. Dev Biol 160: 315–332

Chou T-B, Perrimon N (1992) Use of a yeast site-specific recombinase to produce female germline chimeras in *Drosophila*. Genetics 131: 643–653

Cohen SM (1993) Imaginal disc development. In: Bate M, Martinez Arias A (eds) The development of *Drosophila melanogaster*, Vol. 2. Cold Spring Harbor Press, New York, pp 747–841

Cohen SM, Jürgens G (1989) Proximal-distal pattern formation in *Drosophila:* graded requirement for *Distal-less* gene activity during limb development. Roux's Arch Dev Biol 198: 157–169

Collins MKL, Perkins GR, Rodriguez-Tarduchy G, Nieto MA, López-Rivas A (1994) Growth factors as survival factors: regulation of apoptosis. BioEssays 16: 133–138

Couso JP, Bate M, Martìnez-Arias A (1993) A *wingless*-dependent polar coordinate system in *Drosophila* imaginal discs. Science 259: 484–489

Cross M, Dexter TM (1991) Growth factors in development, transformation, and tumorigenesis. Cell 64: 271–280

Diaz-Benjumea FJ, Cohen SM (1994) *wingless* acts through the *shaggy/zeste-white 3* kinase to direct dorsal-ventral axis formation in the *Drosophila* leg. Development 120: 1661–1670

Diaz-Benjumea FJ, Cohen B, Cohen SM (1994) Cell interaction between compartments establishes the proximal-distal axis of *Drosophila* legs. Nature 372: 175–179

French V, Daniels G (1994) The beginning and the end of insect limbs. Curr Biol 4: 34–37

French V, Bryant PJ, Bryant SV (1976) Pattern regulation in epimorphic fields. Science 193: 969–981

Fristrom D, Fristrom JW (1975) The mechanism of evagination of imaginal discs of *Drosophila melanogaster*. I. General considerations. Dev Biol 43: 1–23

Gelbart WM (1989) The *decapentaplegic* gene: a TGF-β homologue controlling pattern formation in *Drosophila*. Development 1989 (Suppl): 65–74

Girton JR (1981) Pattern triplications produced by a cell-lethal mutation in *Drosophila*. Dev Biol 84: 164–172

Girton JR (1982) Genetically induced abnormalities in *Drosophila*: two or three patterns? Am Zool 22: 65–77

Girton JR, Berns MW (1982) Pattern abnormalities induced in *Drosophila* imaginal discs by an ultraviolet laser microbeam. Dev Biol 91: 73–77

Girton JR, Kumor AL (1985) The role of cell death in the induction of pattern abnormalities in a cell-lethal mutation of *Drosophila*. Dev Genet 5: 93–102

Golic KG (1991) Site-specific recombination between homologous chromosomes in *Drosophila*. Science 252: 958–961

González F, Swales L, Bejsovec A, Skaer H, Martinez Arias A (1991) Secretion and movement of *wingless* protein in the epidermis of the *Drosophila* embryo. Mech Dev 35: 43–54

Goto S, Tanimura T, Hotta Y (1995) Enhancer-trap detection of expression patterns corresponding to the polar coordinate system in the imaginal discs of *Drosophila melanogaster*. Roux's Arch Dev Biol 204: 378–391

Graves BJ, Schubiger G (1982) Cell cycle changes during growth and differentiation of imaginal leg discs in *Drosophila melanogaster*. Dev Biol 93: 104–110

Grimshaw PH (1905) On the terminology of the leg-bristles of Diptera. Entomol Mon Mag 41: 173–176

Hannah-Alava A (1958) Morphology and chaeotaxy of the legs of *Drosophila melanogaster*. J Morphol 103: 281–310

Haynie JL, Bryant PJ (1977) The effects of X-rays on the proliferation dynamics of cells in the imaginal wing disc of *Drosophila melanogaster*. Wilhelm Roux' Arch Entwicklungsmech Org 183: 85–100

Held LI Jr (1979a) Pattern as a function of cell number and cell size on the second-leg basitarsus of *Drosophila*. Wilhelm Roux' Arch Entwicklungsmech Org 187: 105–127

Held LI Jr (1979b) A high-resolution morphogenetic map of the second-leg basitarsus in *Drosophila melanogaster*. Wilhelm Roux' Arch Entwicklungsmech Org 187: 129–150

Held LI Jr (1990) Sensitive periods for abnormal patterning on a leg segment in *Drosophila melanogaster*. Roux's Arch Dev Biol 199: 31–47

Held LI Jr (1995) Axes, boundaries and coordinates: the ABCs of fly leg development. BioEssays 17: 721–732

Held LI Jr, Duarte CM, Derakhshanian K (1986) Extra tarsal joints and abnormal cuticular polarities in various mutants of *Drosophila melanogaster*. Roux's Arch Dev Biol 195: 145–157

Held LI Jr, Heup MA, Sappington JM, Peters SD (1994) Interactions of *decapentaplegic*, *wingless*, and *Distal-less* in the *Drosophila* leg. Roux's Arch Dev Biol 203: 310–319

Hursh DA, Padgett RW, Gelbart WM (1993) Cross regulation of *decapentaplegic* and *Ultrabithorax* transcription in the embryonic visceral mesoderm of *Drosophila*. Development 117: 1211–1222

James AA, Bryant PJ (1981) Mutations causing pattern deficiencies and duplications in the imaginal wing disc of *Drosophila melanogaster*. Dev Biol 85: 39–54

Jiang J, Struhl G (1995) Protein kinase A and Hedgehog signaling in *Drosophila* limb development. Cell 80: 563–572

Kauffman SA, Ling E (1981) Regeneration by complementary wing disc fragments of *Drosophila melanogaster*. Dev Biol 82: 238–257

Klingensmith J, Nusse R (1994) Signaling by *wingless* in *Drosophila*. Dev Biol 166: 396–414

Klingensmith J, Nusse R, Perrimon N (1994) The *Drosophila* segment polarity gene *dishevelled* encodes a novel protein required for response to the *wingless* signal. Genes Dev 8: 118–130

Lawrence PA, Johnston P, Morata G (1986) Methods of marking cells. In: Roberts DB (ed) *Drosophila*: A practical approach. IRL, Oxford, pp 229–242

Lawrence PA, Struhl G, Morata G (1979) Bristle patterns and compartment boundaries in the tarsi of *Drosophila*. J Embryol Exp Morphol 51: 195–208

Lee L-W, Gerhart JC (1973) Dependence of transdetermination frequency on the developmental stage of cultured imaginal discs of *Drosophila melanogaster*. Dev Biol 35: 62–82

Li W, Ohlmeyer JT, Lane ME, Kalderon D (1995) Function of protein kinase A in hedgehog signal transduction and *Drosophila* imaginal disc development. Cell 80: 553–562

Lindsley DL, Zimm GG (1992) The genome of *Drosophila melanogaster*. Academic Press, New York

Mardon G, Solomon N.M, Rubin GM (1994) *dachshund* encodes a nuclear protein required for normal eye and leg development in *Drosophila*. Development 120: 3473–3486

Masucci JD, Miltenberger RJ, Hoffmann FM (1990) Pattern-specific expression of the *Drosophila decapentaplegic* gene in imaginal discs is regulated by 3′ *cis*-regulatory elements. Genes Dev 4: 2011–2023

Meinhardt H (1980) Cooperation of compartments for the generation of positional information. Z Naturforsch 35c: 1086–1091

Meinhardt H (1983) Cell determination boundaries as organizing regions for secondary embryonic fields. Dev Biol 96: 375–385

Morata G, Lawrence PA (1977) The development of *wingless*, a homeotic mutation of *Drosophila*. Dev Biol 56: 227–240

Morata G, Ripoll P (1975) *Minutes*: mutants of *Drosophila* autonomously affecting cell division rate. Dev Biol 42: 211–221

Morimura S, Maves L, Hoffmann FM (1996) *decapentaplegic* overexpression affects *Drosophila* wing and leg imaginal disc development and *wingless* expression. Dev Biol 177: 136–151

Nellen D, Burke R, Struhl G, Basler K (1996) Direct and long-range action of a DPP morphogen gradient. Cell 85: 357–368

Nusse R, Varmus HE (1992) *Wnt* genes. Cell 69: 1073–1087

Orenic TV, Held LI Jr, Paddock SW, Carroll SB (1993) The spatial organization of epidermal structures: *hairy* establishes the geometrical pattern of *Drosophila* leg bristles by delimiting the domains of *achaete* expression. Development 118: 9–20

Padgett RW, St. Johnston RD, Gelbart WM (1987) A transcript from a *Drosophila* pattern gene predicts a protein homologous to the transforming growth factor-β family. Nature 325: 81–84

Panganiban GEF, Reuter R, Scott MP, Hoffmann FM (1990) A *Drosophila* growth factor homolog, *decapentaplegic*, regulates homeotic gene expression within and across germ layers during midgut morphogenesis. Development 110: 1041–1050

Papageorgiou S (1989) Cartesian or polar co-ordinates in pattern formation? J Theor Biol 141: 281–283

Peifer M, Wieschaus E. (1990). The segment polarity gene *armadillo* encodes a functionally modular protein that is the *Drosophila* homolog of human plakoglobin. Cell 63: 1167–1178

Peifer M, Rauskolb C, Williams M, Riggleman B, Wieschaus E (1991) The segment polarity gene *armadillo* interacts with the *wingless* signalling pathway in both embryonic and adult pattern formation. Development 111: 1029–1043

Peifer M, Pai L-M, Casey M (1994a) Phosphorylation of the *Drosophila* adherens junction protein armadillo: roles for wingless signal and zeste-white 3 kinase. Dev Biol 166: 543–556

Peifer M, Sweeton D, Casey M, Wieschaus E (1994b) *wingless* signal and zeste-white 3 kinase trigger opposing changes in the intracellular distribution of armadillo. Development 120: 369–380

Penton A, Hoffmann FM (1996) Decapentaplegic restricts the domain of *wingless* during *Drosophila* limb patterning. Nature 382: 162–165

Poodry CA, Schneiderman HA (1970) The ultrastructure of the developing leg of *Drosophila melanogaster*. Wilhelm Roux' Arch Entwicklungsmech Org 166: 1–44

Posakony LG, Raftery LA, Gelbart WM (1991) Wing formation in *Drosophila melanogaster* requires *decapentaplegic* gene function along the anterior-posterior compartment boundary. Mechs Dev 33: 69–82

Postlethwait JH (1978) Clonal analysis of *Drosophila* cuticular patterns. In: Ashburner M, Wright TRF (eds) The genetics and Biology of *Drosophila*, Vol. 2c. Academic Press, New York, pp 359–441

Postlethwait JH, Schneiderman HA (1973) Pattern formation in imaginal discs of *Drosophila melanogaster* after irradiation of embryos and young larvae. Dev Biol 32: 345–360

Raftery LA, Sanicola M, Blackman RK, Gelbart WM (1991) The relationship of *decapentaplegic* and *engrailed* expression in *Drosophila* imaginal discs: do these genes mark the anterior-posterior compartment boundary? Development 113: 27–33

Ruel L, Pantesco V, Lutz Y, Simpson P, Bourouis M (1993) Functional significance of a family of protein kinases encoded at the *shaggy* locus in *Drosophila*. EMBO J 12: 1657–1669

Russell MA (1985) Positional information in imaginal discs: A Cartesian coordinate model. In: Antonelli PL (ed) Mathematical essays on growth and the emergence of form. University of Alberta Press, Edmonton, pp 169–183

Sanicola M, Sekelsky J, Elson S, Gelbart WM (1995) Drawing a stripe in *Drosophila* imaginal discs: negative regulation of *decapentaplegic* and *patched* expression by *engrailed*. Genetics 139: 745–756

Schubiger G (1968) Anlageplan, Determinationszustand und Transdeterminationsleistungen der männlichen Vorderbein-

scheibe von *Drosophila melanogaster*. Wilhelm Roux' Arch Entwicklungsmech Org 160: 9–40
Schubiger G (1971) Regeneration, duplication and transdetermination in fragments of the leg disc of *Drosophila melanogaster*. Dev Biol 26: 277–295
Siegfried E, Perrimon N (1994) *Drosophila* wingless: a paradigm for the function and mechanism of Wnt signalling. BioEssays 16: 395–404
Siegfried E, Perkins LA, Capaci TM, Perrimon N (1990) Putative protein kinase product of the *Drosophila* segment-polarity gene *zeste-white 3*. Nature 345: 825–829
Spencer FA (1984) The decapentaplegic gene complex and adult pattern formation in *Drosophila*. Ph.D. dissertation, Harvard University
Spencer FA, Hoffmann FM, Gelbart WM (1982) Decapentaplegic: A gene complex affecting morphogenesis in *Drosophila melanogaster*. Cell 28: 451–461
St. Johnston RD, Hoffmann FM, Blackman RK, Segal D, Grimaila R, Padgett RW, Irick HA, Gelbart WM (1990) Molecular organization of the *decapentaplegic* gene in *Drosophila melanogaster*. Genes Dev 4: 1114–1127
Steiner E (1976) Establishment of compartments in the developing leg imaginal discs of *Drosophila melanogaster*. Wilhelm Roux's Arch Entwicklungsmech Org 180: 9–30
Stern C (1936) Somatic crossing over and segregation in *Drosophila melanogaster*. Genetics 21: 625–730
Struhl G, Basler K (1993) Organizing activity of wingless protein in *Drosophila*. Cell 72: 527–540
Tabata T, Schwartz C, Gustavson E, Ali Z, Kornberg TB (1995) Creating a *Drosophila* wing de novo, the role of *engrailed*, and the compartment border hypothesis. Development 121: 3359–3369
Theisen H, Purcell J, Bennett M, Kansagara D, Syed A, Marsh JL (1994) *dishevelled* is required during *wingless* signaling to establish both cell polarity and cell identity. Development 120: 347–360
Tokunaga C (1962) Cell lineage and differentiation on the male foreleg of *Drosophila melanogaster*. Dev Biol 4: 489–516
Villano JL, Katz FN (1995) *four-jointed* is required for intermediate growth in the proximal-distal axis in *Drosophila*. Development 121: 2767–2777
Wilder EL, Perrimon N (1995) Dual functions of *wingless* in the *Drosophila* leg imaginal disc. Development 121: 477–488
Williams JA, Paddock SW, Carroll SB (1993) Pattern formation in a secondary field: a hierarchy of regulatory genes subdivides the developing *Drosophila* wing disc into discrete subregions. Development 117: 571–584
Winfree AT (1980) The geometry of biological time. Springer, Berlin Heidelberg New York
Wolpert L (1969). Positional information and the spatial pattern of cellular differentiation. J Theor Biol 25: 1–47
Xu T, Rubin GM (1993) Analysis of genetic mosaics in developing and adult *Drosophila* tissues. Development 117: 1223–1237
Yanagawa S, Leeuwen F van, Wodarz A, Klingensmith J, Nusse R (1995) The Dishevelled protein is modified by Wingless signalling in *Drosophila*. Genes Dev 9: 1087–1097

Note added in proof

Additional evidence for the mutual antagonism between dpp and wg gene function in leg development has recently been published by Jiang and Struhl (1996) in Cell 86: 401–409 and by Brook and Cohen (1996) in Science 273: 1373–1377